



King Saud University

Arabian Journal of Chemistry

www.ksu.edu.sa  
www.sciencedirect.com



## ORIGINAL ARTICLE

# Conversion of Fe-rich sludge to $KFeS_2$ cluster: Spontaneous hydrolysis of $KFeS_2$ for the effective adsorption of doxycycline



Yu Chen <sup>a,b</sup>, Zhihua Wang <sup>a</sup>, Dongxu Liang <sup>a</sup>, Yanwen Liu <sup>a</sup>, Hongbin Yu <sup>a</sup>,  
Suiyi Zhu <sup>a,b,\*</sup>, Leilei Zhang <sup>a</sup>

<sup>a</sup> Science and Technology Innovation Center for Municipal Wastewater Treatment and Water Quality Protection, Northeast Normal University, Changchun 130117, China

<sup>b</sup> Jilin Province Key Laboratory of Municipal Wastewater Treatment, Changchun Institute of Technology, Changchun 130117, China

Received 27 January 2021; accepted 14 April 2021

Available online 26 April 2021

## KEYWORDS

Fe-bearing precipitates;  
Hydrothermal conversion;  
 $KFeS_2$ ;  
Adsorption;  
Doxycycline

**Abstract** Fe-rich sludge is a solid waste considerably generated in coagulation, Fenton, and catalytic processes for wastewater treatment, in which it is commonly disposed in landfills. However, a limited portion of sludge is recycled as polymeric ferric flocculant and iron red. Herein, the Fe-rich sludge was simulated by the hydrolysis of  $FeCl_3$  and converted to a new one-dimensional  $KFeS_2$  cluster via a one-step hydrothermal route with the addition of  $K_2S$  and  $KOH$ . The results showed that in the hydrothermal process,  $KFeS_2$  cluster grew radially from 2  $\mu m$  to 10  $\mu m$  with the increase in  $KOH$  concentration from 2 M to 5 M. The new cluster showed a high adsorption capacity of 2933.6 mg/L for doxycycline, which is 14 times that of sludge and higher than that of hematite nanoparticles, commercial polymeric ferric flocculant and pyrite. The adsorption isotherm complied with the Langmuir model, and the adsorption kinetics fitted well with the pseudo-second-order model. During adsorption,  $KFeS_2$  cluster was completely hydrolysed to release Fe/S-bearing colloids with a considerable number of Fe-SH/Fe-OH groups for the coordination of the  $-NH_2$  group of tetracycline-type antibiotics, e.g. doxycycline. However, an inefficient removal of quinoline and p-nitrophenol was observed. With the proposed method, the used alkaline solution was completely recycled in the next round of  $KFeS_2$  synthesis without the generation of secondary waste. Such green method has potential applications in the resource utilisation of Fe-rich sludge.

© 2021 The Author(s). Published by Elsevier B.V. on behalf of King Saud University. This is an open access article under the CC BY-NC-ND license (<http://creativecommons.org/licenses/by-nc-nd/4.0/>).

\* Corresponding author at: Science and Technology Innovation Center for Municipal Wastewater Treatment and Water Quality Protection, Northeast Normal University, Changchun 130117, China.

E-mail address: [papermanuscript@126.com](mailto:papermanuscript@126.com) (S. Zhu).

Peer review under responsibility of King Saud University.



Production and hosting by Elsevier

<https://doi.org/10.1016/j.arabjc.2021.103173>

1878-5352 © 2021 The Author(s). Published by Elsevier B.V. on behalf of King Saud University.

This is an open access article under the CC BY-NC-ND license (<http://creativecommons.org/licenses/by-nc-nd/4.0/>).

## 1. Introduction

Fe-bearing reagents, e.g. ferrous sulfate, nanoscale zero-valent iron and polymeric ferric sulfate (PFS), are commonly applied to remove contaminants from water (Ahmad et al., 2016, EPA, 2011, Li et al., 2014, Li et al., 2020a,b, Mooheng and Phenrat, 2019, Qiang et al., 2003, Zhang et al., 2019a,b). The use of such reagents generates the waste Fe-bearing sludge during mass production, with Fe content of 7.5 wt% to 45.6 wt% (Zhu et al., 2015, Zhu et al., 2020a,b), and major impurities, including Ca, Al and Si. About 25 mg/L PFS is added in a surface water plant with the project scale of 7000 m<sup>3</sup>/day, with > 3 t/day sludge generated (EPA, 2011). Such waste sludge has a water content of 95–99.5% and is commonly categorised as a solid waste, followed by mechanical dewatering with the addition of cement and/or pitch before safety landfill, which is tedious and costly. In underdeveloped areas, the direct discharge of sludge into lakes and/or rivers also occurs, where the release of Fe from the sludge to water pollutes the water resources nearby (Osman and Iqbal, 2014). Therefore, a renewable route for the effective treatment of such Fe-bearing sludge should be proposed to reduce the disposal cost and control pollution.

The resource utilisation of sludge as an adsorbent for wastewater treatment is a desirable route. The sludge is rich in surface hydroxyl groups and applied as an adsorbent for the removal of contaminants, e.g. heavy metals (Ngatenah et al., 2010), antibiotics (Sun et al., 2019, Zhu et al., 2020a,b) and organic dyes (Zhu et al., 2015). In the sludge, Fe exists in the form of weakly crystallised compound, which can be converted into magnetite (Zhu et al., 2015), maghemite (Qu et al., 2019) and jacobsonite (Zhu et al., 2019a,b), after hydrothermal treatment and/or calcination. The prepared product exhibits good magnetic response and can be magnetically recycled after use. However, this sludge aggregates, and after conversion into a magnetic adsorbent, the aggregates enlarge due to the dihydroxylation reaction of adjacent Fe-bearing microcrystals (Qu et al., 2019, Zhu et al., 2015, Zhu et al., 2019a,b). Thus, the sludge and the corresponding magnetic adsorbent exhibit a normal performance in the adsorption of contaminants from wastewater. Another utilisation route is to recycle the sludge as flocculant. After the sludge is dissolved in strong acids, e.g. sulfuric and hydrochloric acids, free Fe<sup>2+</sup>/Fe<sup>3+</sup> and Al/Si impurities are released into the acid solution, where the precursor of Fe-bearing flocculant is produced (Li et al., 2020a,b, Mooheng and Phenrat, 2019). Li et al., reported the treatment of Fe-bearing sludge with Fe content of 15.5 wt % by leaching with concentrated hydrochloric acid followed by rotary evaporation, neutralisation and dilution; the prepared FeCl<sub>3</sub> flocculants met the product standards (Li et al., 2020a,b). The Fe-bearing flocculant is hydrolysed and polymerised to form flocs and exhibits sufficient surface groups of Fe-OH to coordinate contaminants in the wastewater treatment. The drawback is the rapid hydrolysis of Fe as aggregates, resulting in a low removal efficiency.

Recently, a new erdite-bearing product was synthesised with Fe-bearing sludge as the raw material (Qu et al., 2020), and it showed an ideal capability for the adsorption of tetracycline (Hu et al., 2020, Zhu et al., 2019a,b), Zn and Cu (Liu et al., 2020). In the new product, erdite has a special structure in which one Fe atom is covalent with four S atoms to form

rod-shaped particles (Honma et al., 2003). The special Fe-S structure of erdite is stable in alkaline condition (Lassin et al., 2014), decomposes in neutral solutions to generate small Fe/S-bearing flocs and uses plenty of surface coordination sites for contaminant adsorption. KFeS<sub>2</sub> exists in the form of a linear chain with an Fe/S-bearing structure and exhibits desirable application in the recycling of Fe-bearing sludge, similar to erdite. In the past, KFeS<sub>2</sub> was used as a common reagent to prepare electrode materials in the battery industry (Guy et al., 2008, Han et al., 2020); however, the application of KFeS<sub>2</sub> in wastewater treatment has not been reported. Notably, three important aspects should be considered in investigations to recycle the Fe-bearing sludge as KFeS<sub>2</sub>. First, the formation possibility of KFeS<sub>2</sub> in the sludge should be investigated. Second, studies should analyse whether ferrous-bearing compounds in the sludge are involved in KFeS<sub>2</sub> formation because Fe<sup>2+</sup> is commonly coprecipitated with Fe<sup>3+</sup> in sludge during coagulation, demulsification and Fenton processes (EPA, 2011, Qiang et al., 2003). Third, the hydrolysis of KFeS<sub>2</sub> in the wastewater treatment must be verified.

Doxycycline is a common antibiotics in pharmaceutical effluents (Zaidi et al., 2019), and it is targeted as a typical contaminant to analyse the adsorption capacity of KFeS<sub>2</sub>. This compound can inhibit bacterial protein synthesis by binding to a ribosomal subunit to stop bacteria from reproducing (Chukwudi and Good, 2019). The high-value discharge of doxycycline into the environment results from antibiotic production, mainly via the continuous discharge of effluents from wastewater stations (Bousek et al., 2018, Álvarez-Esmoris et al., 2020, Zaidi et al., 2019). Although doxycycline is not closely associated with harm to the environment, recent concerns emerged regarding the antimicrobial resistance and its chronic effects on biodiversity (Chukwudi and Good, 2019, Neth et al., 2017). Hence, the effective removal of doxycycline and its derivatives from wastewater is currently of great interest to the manufacturer and water industries alike, with a focus on the intensive regulation of the water environment.

In this paper, the Fe-bearing sludge from the coagulation process was simulated and converted into the KFeS<sub>2</sub>-bearing adsorbent. The formation mechanism of KFeS<sub>2</sub> was analysed, and the performance of KFeS<sub>2</sub> hydrolysis in doxycycline-bearing wastewater was investigated.

## 2. Materials and methods

### 2.1. Laboratory simulation of Fe-rich sludge

The Fe-rich sludge was produced by mixing 162 g FeCl<sub>3</sub> in 5000 mL deionised water to form a transparent solution, followed by adjusting to pH 9 by KOH. Afterwards, a brownish sludge was precipitated at the bottom of the water and collected through suction filtration by using a filter paper. A small portion of the sludge was freeze-dried at –80 °C overnight for characterisation. Another sludge was kept in a beaker and sealed with a parafilm for the KFeS<sub>2</sub> preparation.

### 2.2. Hydrothermal preparation of KFeS<sub>2</sub>

About 5 mL sludge was sampled using 5 mL injection syringe and then injected into 30 mL liquid containing 2 M KOH and 1 M K<sub>2</sub>S to produce a mixture. Subsequently, the mixture was

agitated for 5 min at 90 rpm and dumped into a Teflon vessel, followed by heating at 120 °C for 15 h. Afterward, black particles were formed at the vessel bottom. These particles were transferred to a plastic tube and placed in a lyophiliser (FDU-2200, EYELA, Japan) for drying at -80 °C for 24 h. The dried particles were denoted as P2. A control experiment was performed using the abovementioned method except for the increase in the KOH concentration from 2 M to 5 M. The corresponding particles were named as P5.

### 2.3. Application of KFeS<sub>2</sub> in doxycycline removal

Doxycycline was targeted as the model organic pollutant to determine the adsorption performance of synthesised KFeS<sub>2</sub>-bearing products. Doxycycline is a hydrophilic molecule of C<sub>22</sub>H<sub>24</sub>N<sub>2</sub>O<sub>8</sub> with a molar mass of 444 g/mol and a low log *K<sub>ow</sub>* value of -0.02 (Álvarez-Esmoris et al., 2020). However, this compound is amphoteric with three *pK<sub>a</sub>* values of 3.5, 7.7 and 9.5 (Brigante and Avena, 2016). At a low pH (<3.5), doxycycline was fully protonated as DCH<sub>3</sub><sup>+</sup> (Fig. 1). With the pH increase, deprotonation reaction occurred at the hydroxyl groups of the C-3 position to form zwitterionic DCH<sub>2</sub><sup>±</sup>. When the solution pH was higher than 7.7, the deprotonation step continued at the hydroxyl groups of O-10/O-12 ketophenolic position to form negative DCH<sup>-</sup>. However, at a high pH of 9.5, the final deprotonated step involved the dimethylamino group with the generation of negative DC<sup>2-</sup> (Gao et al., 2012).

The adsorption experiment was performed as follows. In brief, 0.2 g raw sludge was dispersed in a solution containing 10 mg/L doxycycline, followed by shaking at 60 rpm for 2 h. Afterwards, the added sludge was separated. About 1 mL supernatant was collected, and the doxycycline concentration in the supernatant was detected by high-performance liquid chromatography (LC-16, Shimadzu, Japan). Control experiments were performed by varying the doxycycline concentrations (10–2000 mg/L) following the above steps, and accordingly, the maximum adsorption capacity (*q<sub>m</sub>*) of raw sludge was determined. The raw sludge was replaced with P2 and P5 to determine the *q<sub>m</sub>* values of P2 and P5, respectively.

## 3. Results and discussion

### 3.1. KFeS<sub>2</sub> cluster growth in the presence of KOH

The raw sludge was an irregular block with Fe content of 31.4 wt% and showed weak peaks of FeOOH, revealing that Fe oxides were weakly crystallised in the sludge. When the sludge was treated with the addition of 1 M K<sub>2</sub>S and 2 M KOH, the product P2 was a short rod with 2 μm length and

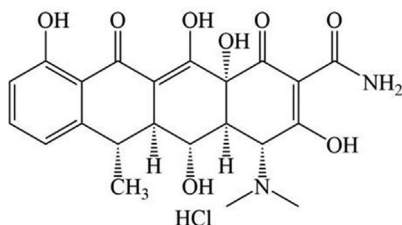


Fig. 1 Molecular structure of protonated doxycycline.

200 nm diameter, respectively, and exhibited sharp peaks of KFeS<sub>2</sub> and hematite, suggesting the conversion of the weakly crystallised FeOOH into KFeS<sub>2</sub> and hematite (Figs. 2 and 3 (a)). With the increment in the KOH concentration from 2 M to 5 M, the prepared P5 exhibited typical KFeS<sub>2</sub> and hematite peaks, but its length grew radially to 10 μm. This finding indicated the radial growth of KFeS<sub>2</sub> rods to clusters at high KOH concentration. However, without KOH, only the peaks of sulphur and pyrite were recorded (Fig. S1), demonstrating that KOH was important for KFeS<sub>2</sub> and hematite formation.

The raw sludge, P2 and P5 were also characterised using XPS (Fig. 3(b) and 3(c)). For the Fe 2p curves, an extensive peak was observed at 710.5 eV, and it belonged to the Fe-O bond of Fe oxides in the sludge (Liu et al., 2020). However, with the addition of KOH, a new peak appeared at 708.4 eV, and it was affiliated to the structural Fe in the (FeS<sub>2</sub>)<sub>n</sub><sup>n-</sup> bond of KFeS<sub>2</sub> (Bronold et al., 1991, Zhang et al., 2019a,b). For the S 2p curves, four peaks at 160.3, 161.2, 163.2 and 167.4 eV belonged to the structural S in (FeS<sub>2</sub>)<sub>n</sub><sup>n-</sup> group (Bronold et al., 1991), S<sup>2-</sup>, elemental S and sulfate, respectively, demonstrating that KFeS<sub>2</sub> was generated from the FeOOH in the sludge (Fig. 3(d)). Fig. 4(a) shows the Raman spectra of the raw sludge, P2 and P5. For the sludge, a strong peak, which is characteristic of FeOOH, appeared at 148 cm<sup>-1</sup> (Dunnwald and Otto, 1989, Gui and Devine, 1993). With hydrothermal treatment, the peak disappeared, whereas two new peaks were observed at 332 and 363–365 cm<sup>-1</sup>. These new peaks corresponded to the symmetry and antisymmetric stretching modes of the Fe-S<sub>4</sub> tetrahedron (Thomas et al., 1970), a characteristic (FeS<sub>2</sub>)<sub>n</sub><sup>n-</sup> structure of KFeS<sub>2</sub>. In addition, two broad peaks at 972 and 1421 cm<sup>-1</sup> were recorded in the two products, and they were assigned to hematite (Gui and Devine, 1993, Mazzetti and Thistlethwaite, 2002). Fig. 4 (b) shows the infrared (IR) spectra of these products. The sludge comprised peaks of the adsorbed/lattice water (1627 cm<sup>-1</sup>), Fe-OH (1014 and 1396 cm<sup>-1</sup>) and stretching of Fe-O (465 cm<sup>-1</sup>) (Liu et al., 2018). After the hydrothermal process, the P2 and P5 spectra showed that the peaks of Fe-O shifted slightly to 466–469 cm<sup>-1</sup>, whereas that of Fe-OH disappeared. A new peak appeared at 547–550 cm<sup>-1</sup>, and it belonged to the stretching vibration of Fe-S bond (Wang et al., 2021), in agreement with the formation of KFeS<sub>2</sub>. Moreover, three new peaks at 998–999, 1127 and 1224–1227 cm<sup>-1</sup> signalled the presence of the adsorbed sulfate (Galembeck and Alves, 1995, Rupa Ranjani et al., 2021). From the transmission electron microscopy (TEM) image in Fig. 5, the low-magnification images confirmed that fibre-sharp particles were distributed in the clusters of P2 and P5. The high-resolution images showed that the particles were highly crystallised with the interplanar distances of 0.564 and 0.282 nm, which matched well with the (020) and (220) facets of KFeS<sub>2</sub> (JCPDS No. 45-1008), respectively, revealing that the fibre-sharp KFeS<sub>2</sub> was generated in P2 and P5.

### 3.2. Formation mechanism of KFeS<sub>2</sub> and hematite

Fe-bearing minerals in the sludge were stable at room temperature and contained numerous surface hydrogel groups. However, at high temperature, the conjunction reaction between the adjacent Fe-OH of the Fe-bearing microcrystal occurred,

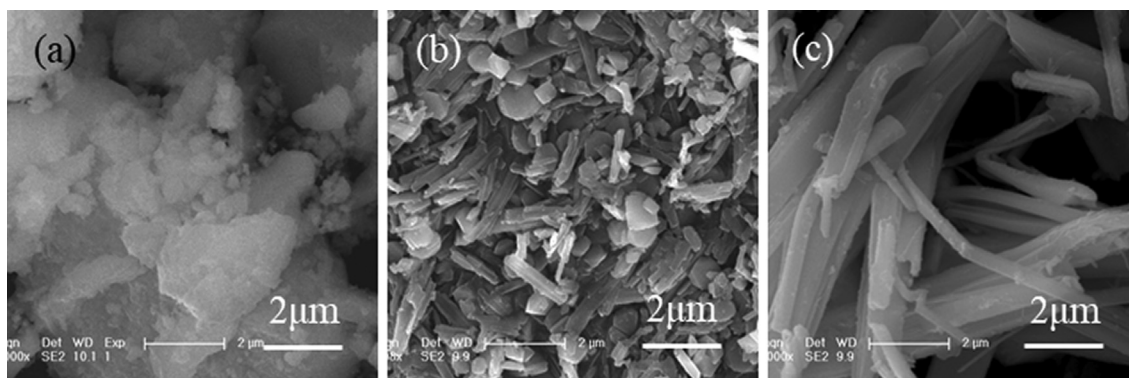


**Fig. 2** Scanning electron microscopy (SEM) images of (a) raw sludge and  $\text{KFeS}_2$  prepared with (b) 2 and (c) 5 M KOH.

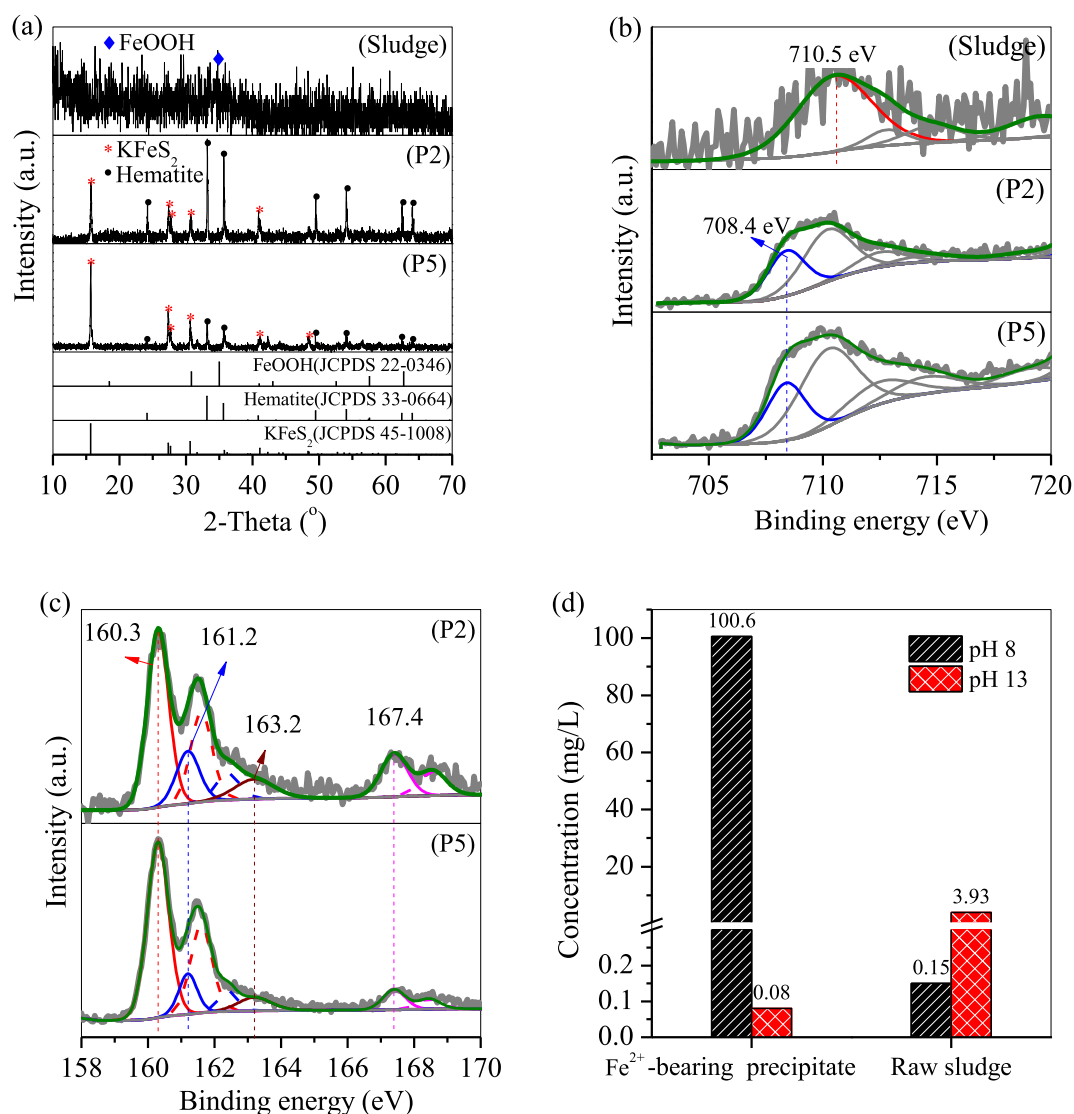


**Fig. 3** (a) X-ray diffraction (XRD) patterns and X-ray photoelectron spectroscopy (XPS) (b) Fe2p and (c) S2p spectra of the raw sludge, P2 and P5 and (d) Fe concentration in the supernatant after dissolution of the raw sludge and  $\text{Fe}^{2+}$ -bearing sludge at pH 8 and 13.

in which a water molecule was released, and a stable Fe-O-Fe bond was formed. Such reaction accelerated with the temper-

ature increase, and thereby, well-crystallised hematite was generated (Fig. 6), leading to the polymerisation of Fe-bearing

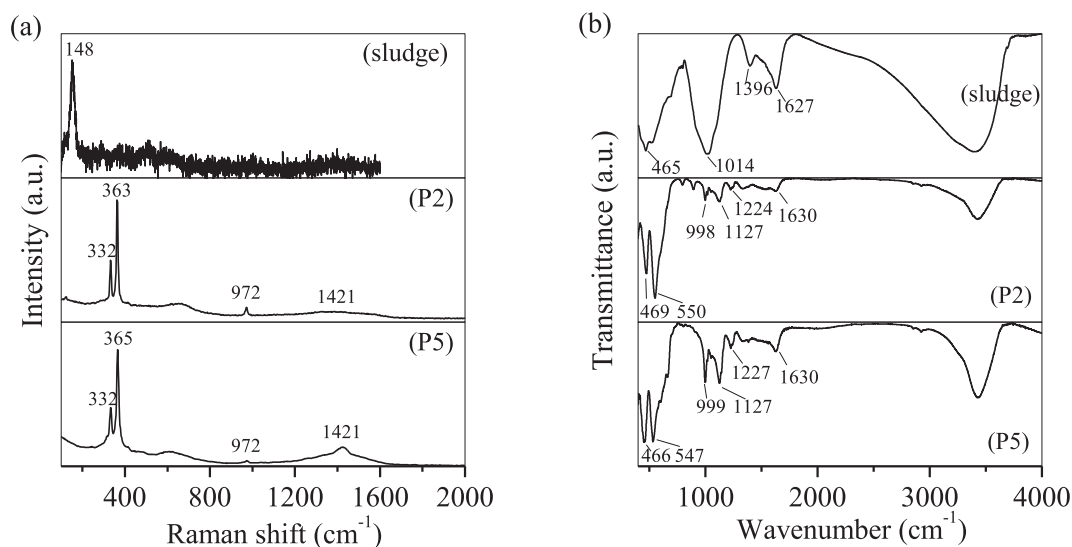


**Fig. 4** (a) Raman and (b) Fourier transform infrared spectroscopy (FTIR) spectra of the sludge, P2 and P5.

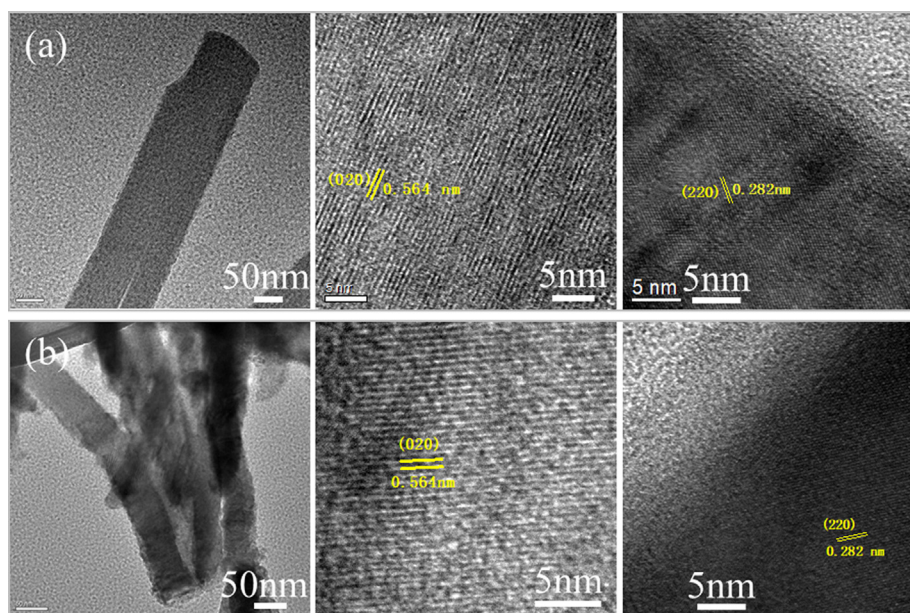


**Fig. 5** TEM images of (a) P2 and (b) P5.

microcrystals. The dehydration in the conjunction reaction intensified at high-alkaline conditions, which accelerated the formation of hematite and the aggregates of sludge particles.

When  $\text{K}_2\text{S}$  and  $\text{KOH}$  were introduced to the hydrothermal system, numerous  $\text{HS}^-$  and  $\text{OH}^-$  were generated, which steadily adjusted the solution to  $\text{pH} > 13.5$ . Consequently, the conversion of  $\text{FeOOH}$  to hematite occurred. However, in the solution, the free  $\text{OH}^-$  diffused to the  $\text{FeOOH}$  surface, where it attacked the surface structural  $\text{Fe}$  of  $\text{FeOOH}$  to generate  $\text{Fe}(\text{OH})_4^-$ . Thereby, free  $\text{Fe}(\text{OH})_4^-$  was released into the solution. Fig. 3(d) shows that 0.15 mg/L  $\text{Fe}$  was produced in the supernatant at  $\text{pH} 8$ , and this phenomenon was affiliated with the dissolution of  $\text{Fe}^{3+}$ -bearing compounds in the raw sludge. However, the  $\text{Fe}$  concentration increased to 3.9 mg/L in the supernatant at  $\text{pH} 13$  due to the formation of  $\text{Fe}(\text{OH})_4^-$ . At

high alkaline solution, the Gibbs energy of  $\text{Fe}(\text{OH})_4^-$  formation at room temperature was  $-201.97$  kcal/mol (Diakonov et al., 1999), in accordance with the spontaneous conversion of  $\text{Fe}$  on the sludge to  $\text{Fe}(\text{OH})_4^-$ . Thus,  $\text{Fe}(\text{OH})_4^-$  was generated continuously. The free  $\text{Fe}(\text{OH})_4^-$  has abundant hydroxyl groups, which can be replaced by  $\text{HS}^-$  to form  $\text{Fe}(\text{OH})_3\text{HS}^-$ . Subsequently, two new  $\text{Fe}(\text{OH})_3\text{HS}^-$  groups were spontaneously polymerised to  $\text{FeS}_2\text{Fe}(\text{OH})_4^-$  with two water molecules released to the solution. As the polymerisation reaction continued, the  $(\text{FeS}_2)_n^-$  group was generated. The free charge was neutralised by free  $\text{K}^+$  in the solution, where the inter-space tunnel was also occupied by free  $\text{K}^+$ , resulting in the  $\text{KFeS}_2$  crystal in the form of one-dimensional rods (Fig. 6). With the increase in  $\text{KOH}$  concentration from 2 M to 5 M, the  $\text{OH}^-$  concentration also increased, which accelerated the

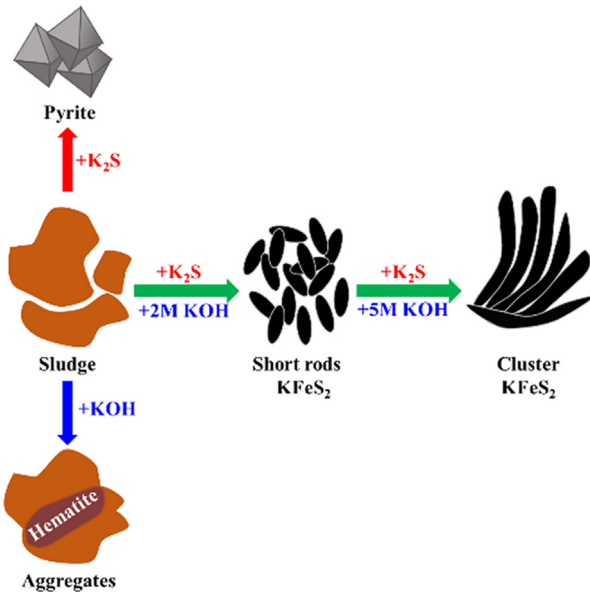


**Fig. 6** Conversion of sludge to  $\text{KFeS}_2$  in the  $\text{K}_2\text{S}/\text{KOH}$ -bearing solution.

generation and the release of  $\text{Fe}(\text{OH})_4^-$  from the sludge surface. Accordingly, the polymerisation reaction proceeded with the supplementation of abundant  $\text{Fe}(\text{OH})_4^-$ , leading to the radial growth of the  $\text{KFeS}_2$  cluster (Fig. 3).

Without the addition of  $\text{KOH}$ , only  $\text{K}_2\text{S}$  was hydrolysed to  $\text{HS}^-$  and  $\text{OH}^-$ , and the solution pH was below 10 after the reaction. A small amount of  $\text{Fe}$  (0.15 mg/L at pH 8) was detected in the solution (Fig. 3(d)), which retarded the formation of the  $\text{KFeS}_2$  crystal. Thus, free  $\text{HS}^-$  was directly diffused to the sludge surface via electronic adsorption, where one electron was transferred from S to structural Fe, which triggered the redox reaction between the Fe of the sludge and  $\text{HS}^-$ , with pyrite being the final product (Fig. 4).

In comparison with the  $\text{Fe}^{3+}$ -bearing sludge, the  $\text{Fe}^{2+}$ -bearing sludge was in the form of an irregular block but did not release high amounts of free  $\text{Fe}$  ( $< 0.1$  mg/L) into the solution (Fig. 3d). After hydrothermal treatment, the  $\text{Fe}^{2+}$ -bearing sludge was converted into a mixture of  $\text{KFeS}_2$ , arcanite,  $2\text{Fe}(\text{OH})\text{SO}_4$  and  $\text{K}_2\text{S}_2\text{O}_3$  in aggregated form (Fig. 7(a) and 7 (b)). In the  $\text{Fe}^{2+}$ -bearing sludge production, dissolved oxygen was present in the solution, and a small portion of  $\text{Fe}^{2+}$  was oxidised to  $\text{Fe}^{3+}$  (Li et al., 2020a,b), and this  $\text{Fe}^{3+}$  was involved in the formation of  $\text{KFeS}_2$ . However, no rod nor cluster was observed (Fig. 7b), demonstrating that the involvement of  $\text{Fe}^{2+}$  in the  $\text{KFeS}_2$  formation was retarded.

### 3.3. Doxycycline adsorption

The sludge and prepared products were employed to adsorb doxycycline (Fig. 8). The adsorption data of doxycycline were fitted by a non-linear Langmuir model, and the relative equation (Eq. (1)) was expressed as follows:

$$q_e = \frac{q_m \times K_L \times C_e}{1 + K_L \times C_e} \quad (1)$$

where  $C_e$  is the equilibrium concentration of doxycycline in the solution (mg/L);  $q_e$  and  $q_m$  are the equilibrium and maximum

adsorption capacity (mg/g), respectively;  $K_L$  is the Langmuir isotherm constants.

Table 1 summarises the adsorption parameters. The regression coefficient ( $R^2$ ) of hematite was 0.928, whereas those of other adsorbents were  $> 0.99$ . This finding confirmed that the sludge, P2, P5 and other three common adsorbents had energetically homogeneous surface for the adsorption of doxycycline.

The raw sludge had a low  $q_m$  of doxycycline (273.2 mg/g), which was approximately 1/14 that of P5 (Fig. 8a). The  $q_m$  of P5 was 2933.6 mg/g, which was slightly high compared with that of P2, suggesting that the radial growth of  $\text{KFeS}_2$  as cluster particles is profitable. Fig. 8b shows that the  $q_m$  of P5 was also higher than those of pyrite (303.9 mg/g), hematite (194.6 mg/g) and PFS (784.6 mg/g). This finding demonstrates that in P2 and P5, the formed  $\text{KFeS}_2$  played a key role in doxycycline adsorption.

P5 showed a desirable adsorption capacity of doxycycline, and accordingly, its adsorption kinetic of doxycycline was also investigated. As shown in Fig. 9, the adsorption data fitted well with the pseudo-second-order model (Eq. (2)), and both the experimental adsorption capacities of doxycycline ( $q_t$ ) were in agreement with the calculated values of pseudo-second-order model (Table 2). Thus, the adsorption of doxycycline on P5 was controlled by chemisorption.

$$q_t = \frac{q_e^2 k_1 t}{1 + q_e k_1 t} \quad (2)$$

where  $q_e$  and  $q_t$  are the adsorption capacity of doxycycline (mg/g) at equilibrium and at any instant time,  $t$ , respectively, and  $k_1$  (L/h) is the rate constant of the pseudo-second-order adsorption model ( $\text{g}/\text{mg h}^{-1}$ ).

The used P5 was regenerated with 15%  $\text{NaCl}$  solution at pH 5 for 48 h (named as Method A) or calcinated at  $450^\circ\text{C}$  for 2 h (named as Method 2). The results showed that P5 was regenerated easily using  $\text{NaCl}$  solution as the desorption agent. However, the removal efficiency of doxycycline decreased to 28.5%. After being calcinated at  $450^\circ\text{C}$ , the regenerated P5 showed a low removal efficiency of doxycycline (53.2%). In addition, with the continued regeneration process, the removal efficiency gradually decreased to 27.1% for the second round and 18.1% for the third round (Fig. 10) due to the aggregation of Fe-bearing compounds in the calcination process. These findings indicate that P5 cannot be feasibly reused.

### 3.4. Characterisation of used $\text{KFeS}_2$ rods

After adsorption, the raw sludge was almost unchanged and showed a weakly crystallised  $\text{FeOOH}$  block (Fig. 11(a) and (b)). However, for P2 and P5, the rod-shaped  $\text{KFeS}_2$  disappeared, and irregular aggregates were observed (Fig. 11(b) and (c)). Accordingly, the sharp peaks of  $\text{KFeS}_2$  were absent, and only peaks of hematite were observed, along with the weak peaks of sulfur from the oxidation of structural S in  $\text{KFeS}_2$  (Fig. 12a). This finding suggests that  $\text{KFeS}_2$  was spontaneously decomposed, and hematite was stable during doxycycline adsorption. The raw sludge, P2 and P5 were also characterised using XPS after adsorption (Fig. 12(b) and 12(c)). For the Fe 2p spectra, the peak of Fe-O bond was also recorded in the sludge spectrum. However, after adsorption, the peak of struc-

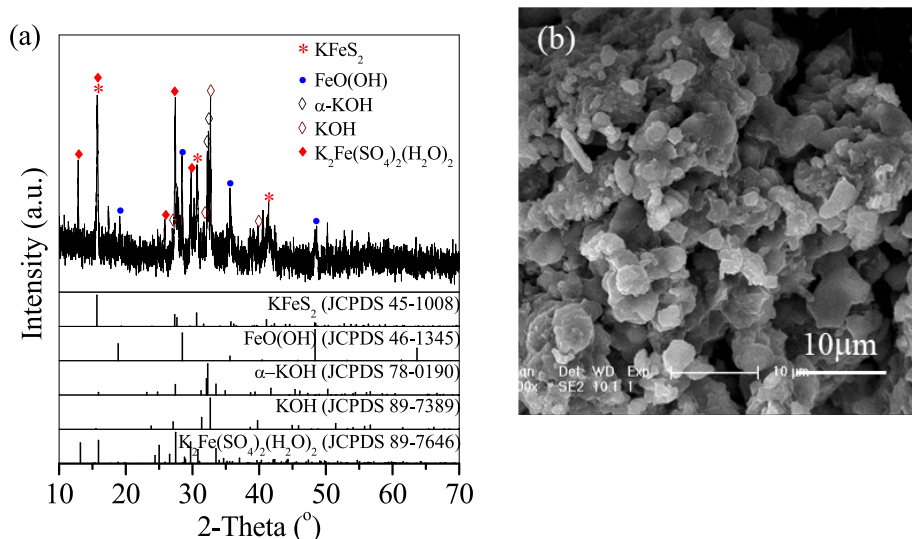


**Fig. 7** (a) XRD pattern and (b) SEM image of the product synthesised with  $\text{Fe}^{2+}$ -bearing sludge.

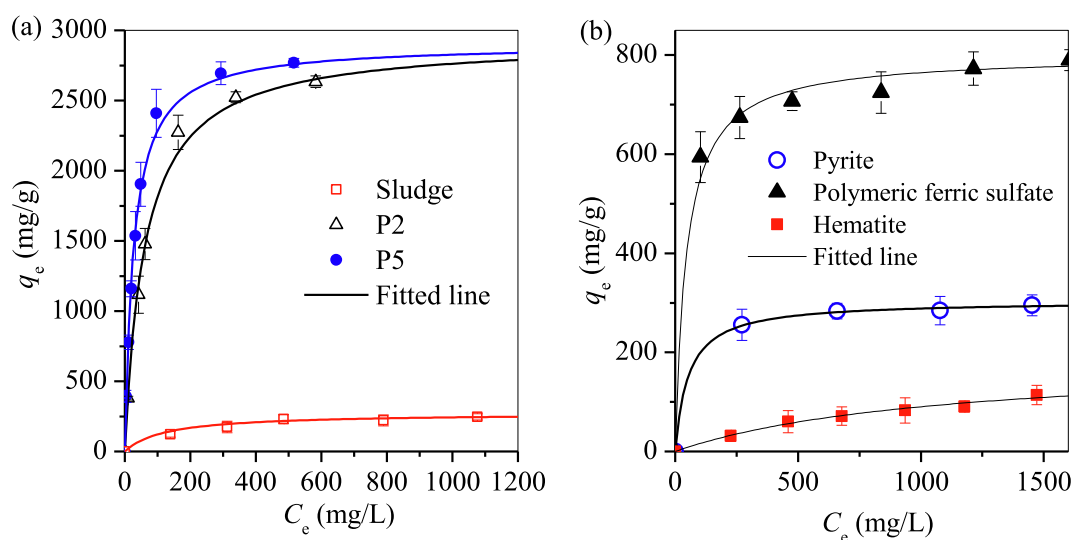


**Fig. 8** Adsorption isotherm of doxycycline by (a) raw sludge, P2 and P5 in comparison with that by (b) pyrite, PFS and hematite particles.

**Table 1** Parameters of doxycycline adsorption on the sludge, P2 and P5.

Model	Parameters	sludge	P2	P5	Pyrite	PFS	hematite
Langmuir	$R^2$	0.993	0.999	0.998	0.999	0.998	0.928
	$q_m$ (mg/g)	273.2	2811.8	2933.6	303.9	784.6	194.6
	$K_L$	0.006	0.037	0.02	0.018	0.017	0.001

tural Fe in the  $(\text{FeS}_2)_n^{n-}$  group in the spectra of P2 and P5 disappeared, in agreement with the decomposition of  $\text{KFeS}_2$ ; a new peak was recorded at 710.2 eV, in reference with the structural Fe in the Fe–S/Fe–O group (Li et al., 2008, Simonetti et al., 2006). For the N 1s spectra, two typical peaks at the binding energies of 399.5 and 402 eV were affiliated to the  $-\text{NH}_2$  group and the  $-\text{N}-$  bond of doxycycline, respectively (Yang et al., 2018). After calculating the relative ratio of peak intensity (short for  $I$ ), the  $I_{402}/I_{399.5}$  of P2 was 0.67, which is

close to that of P5 (0.7). This result indicates that the adsorbed doxycycline on P2 and P5 exhibited a disordered structure, which was conducive to doxycycline adsorption.

The Raman spectra showed that the typical peaks of  $\text{Fe-S}_4$  tetrahedron disappeared in the used P2 and P5 after adsorption (Fig. 13), which was in agreement with the spontaneous hydrolysis of  $\text{KFeS}_2$  in the solution. Moreover, the broad peaks of hematite were not observed. Instead, two tall peaks appeared at 1337–1341 and 1569–1570  $\text{cm}^{-1}$  in the D and G

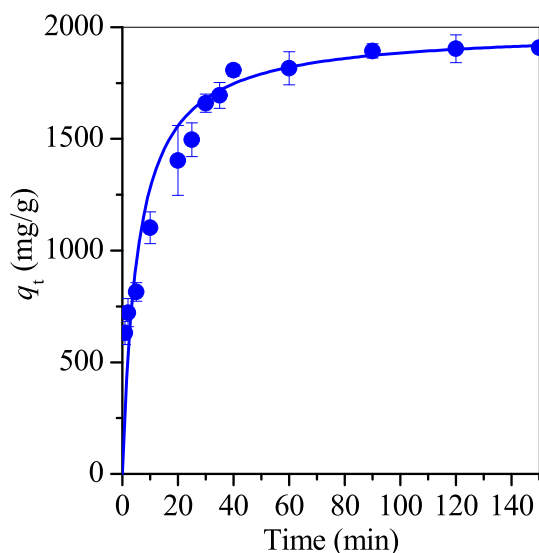


**Fig. 9** Adsorption kinetics of doxycycline on P5. In the figure, the experiment was performed at the doxycycline concentration of 2000 mg/L at the initial pH 5.5.

**Table 2** Parameters of the model for doxycycline adsorption on P5.

Model	Parameters	P5
Pseudo-second-order kinetic	$R^2$	0.997
	$K_1 (\times 10^{-3} \text{ g/mg}\cdot\text{min})$	0.091
	$q_t (\text{mg/g})$	1988.8

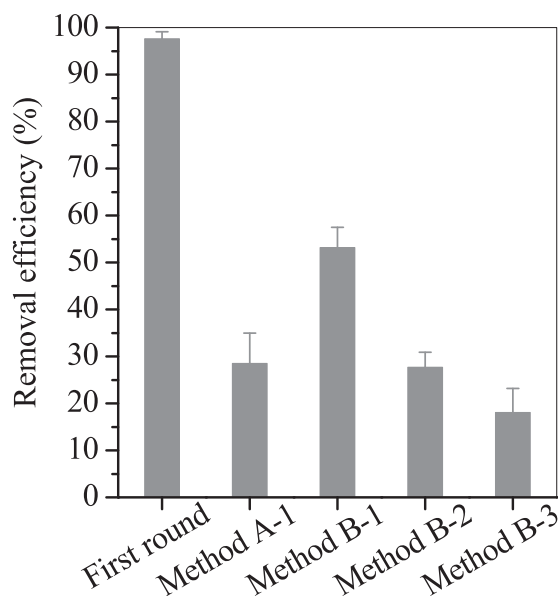


**Fig. 10** Reuse of the precipitate of hydrolysed P5 for doxycycline. In the figure, the experiment was performed at the initial concentration of 2000 mg/L at pH 5.5 at room temperature.

bands, respectively, and they overlapped with the hematite peaks. The D band belonged to the aromatic structure of the  $sp^3$  bonded carbons, whereas the G band was due to first-order scattering of the stretching vibration mode  $E_{2g}$  observed for  $sp^2$  carbon domains. This phenomenon demonstrated the existence of adsorbed doxycycline on hydrolysed  $KFeS_2$  of P2 and P5. The FTIR spectra of P2 and P5 after adsorption displayed peaks at  $470$  and  $550 \text{ cm}^{-1}$ , which demonstrated that Fe-O and/or Fe-S were in the hydrolysed product. The hydrolysed P2 and P5 exhibited adequate -SH bond, which commonly corresponds to the peak of  $1590 \text{ cm}^{-1}$  (Wang et al., 2021). However, after adsorption, the peak shifted slightly to  $1598 \text{ cm}^{-1}$ , probably because of the coordination reaction between the -SH bond and  $-NH_2$  group of doxycycline. In addition, a peak was observed at  $1448\text{--}1450 \text{ cm}^{-1}$ , and it was caused by the bending vibration of  $-CH_3$  in doxycycline (Tang et al., 2021). The peaks of the adsorbed sulfate weakened and shifted to  $1033\text{--}1036$ ,  $1110$  and  $1219\text{--}1221 \text{ cm}^{-1}$ , in accordance with the variation in the adsorption sites of the adsorbed sulfate on the hydrolysed  $KFeS_2$ .

### 3.5. Adsorption mechanism

The sludge comprised weakly crystallised  $FeOOH$ , which had a special structure consisting of one Fe coordinated with 5.2 hydroxyl groups (Jianmin, 1994). Thus, the sludge contained plenty of hydroxyl groups for the coordination of heavy metals and cationic organic compounds (Ngatenah et al., 2010, Zhu et al., 2015, Zhu et al., 2020a,b). Doxycycline occurs in three forms in solutions, namely, cationic at  $pH < 3.5$ , zwitterionic at  $pH 3.5\text{--}7.7$  and anionic at  $pH > 7.7$  (Brigante and Avena, 2016). When the sludge was dispersed in the doxycycline-bearing solution, the zwitterionic doxycycline was attached to the sludge surface, in which the  $-NH_2$  group of doxycycline spontaneously reacted with the hydroxyl group of the sludge, with the generation of stable  $Fe-O-NH_3^+$  ligand. This phenomenon led to the adsorption of doxycycline on the sludge surface. In the conversion of  $FeOOH$  into hematite, the Fe-bearing microcrystals aggregated to produce hematite particles, which decreased the number of functional hydroxyl groups (Jianmin, 1994), whereas hematite showed a low doxycycline adsorption.

In contrast to  $FeOOH$  and hematite, the  $KFeS_2$  was metastable in neutral solution and spontaneously hydrolysed to small rods and further to fine Fe/S-bearing colloid (Fig. 14). The hydrolysis of  $KFeS_2$  occurred slowly in comparison with those of pure  $FeCl_3$  and/or PFS. As shown in Fig. S2(a), hematite and  $KFeS_2$  peaks were observed in the hydrolysed P2 after the doxycycline adsorption for 20 mins, in accordance with the slow hydrolysis of  $KFeS_2$  in the solution. The newly formed product of  $KFeS_2$  was a fine colloid with a hydrodynamic radius of about  $0.5 \mu\text{m}$  (Fig. S2(b)) under constant stirring at 110 rpm, polymerised gradually in the form of flocs after stirring and exhibited abundant Fe-SH/Fe-OH groups. In comparison with the Fe-OH group, the new Fe-SH group was a typical Lewis base and had good affinity to complex with the  $-NH_2$  group of doxycycline because S has a larger atomic radius than O and shows strong electronegativity in the form of  $-S^-$  (Chen et al., 2011, Prashanth et al., 2021). Thus, the flocs exhibited a desirable doxycycline adsorption capacity.

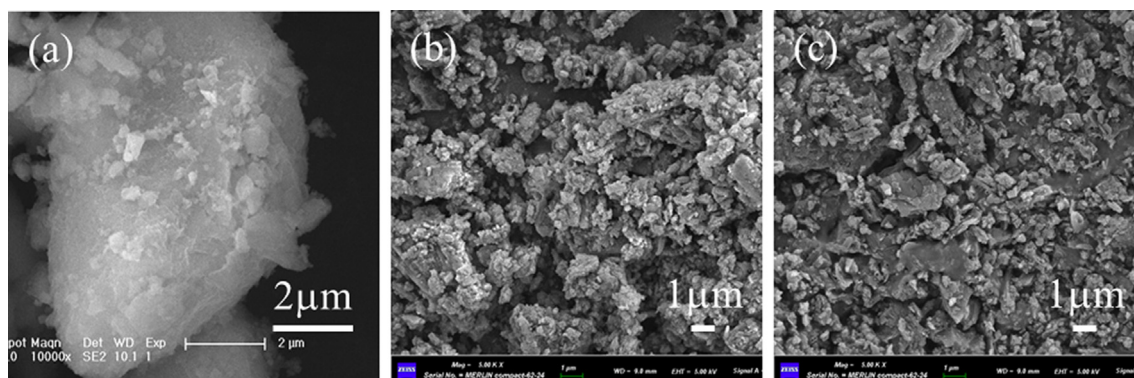


Fig. 11 SEM images of (a) sludge, (b) P2 and (c) P5 after doxycycline adsorption.

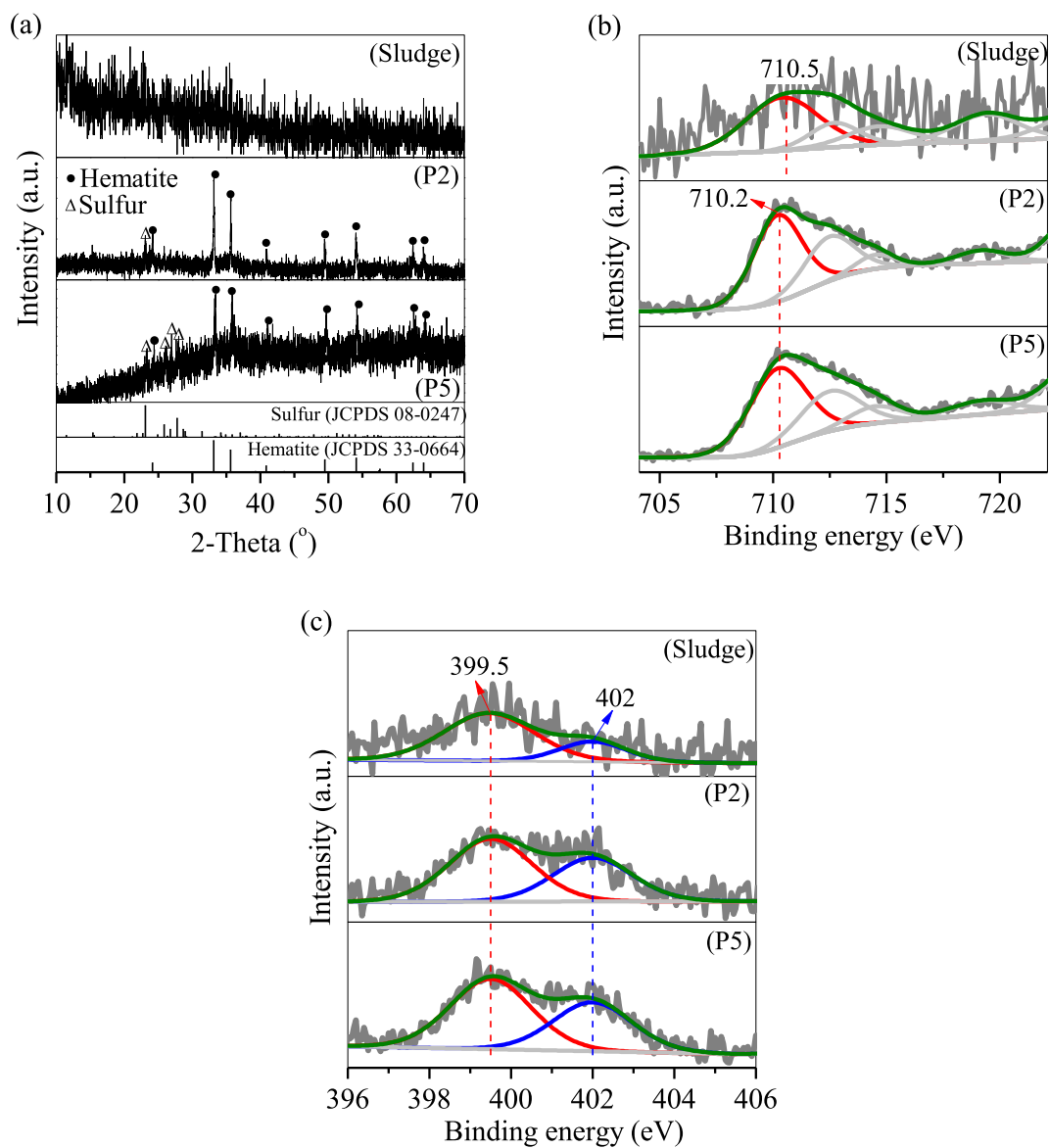
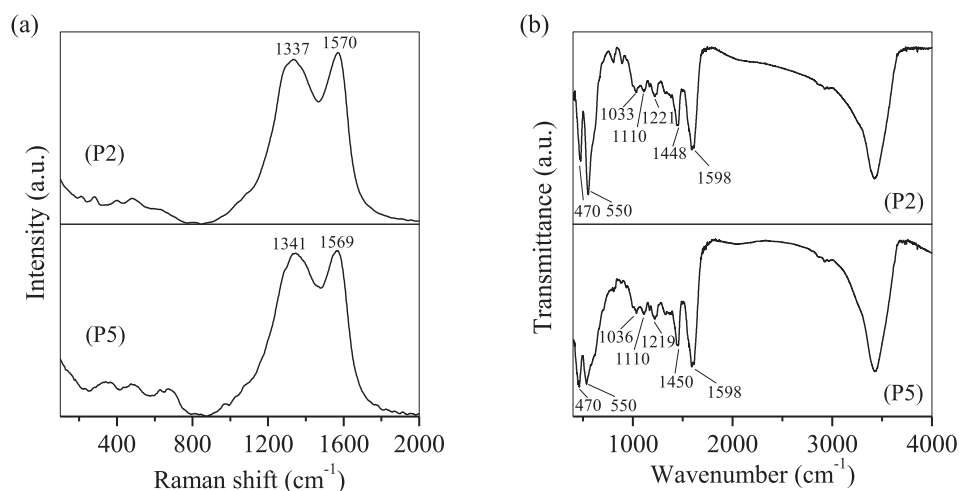
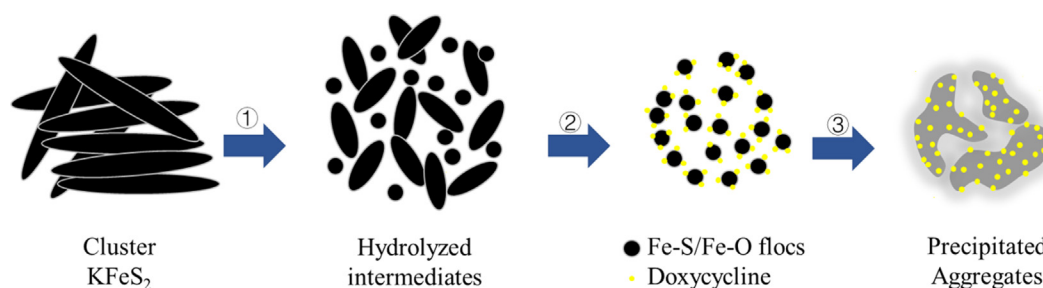


Fig. 12 (a) XRD pattern and XPS (b) Fe 2p and (c) N 1s spectra of the sludge, P2 and P5 after doxycycline adsorption.



**Fig. 13** (a) Raman and (b) FTIR spectra of P2 and P5 after doxycycline adsorption.



**Fig. 14** Possible route of  $\text{KFeS}_2$  rod hydrolysis for doxycycline adsorption.

### 3.6. Potential application in environmental pollution control

The synthesised product P5 showed a higher removal efficiency of doxycycline compared with P2 and the Fe-bearing sludge. Thereby, P5 was applied in the adsorption of quinoline, p-nitrophenol and the derivatives of doxycycline (Fig. 15). The removal efficiency of doxycycline was nearly 100%, similar to those of oxytetracycline, chlortetracycline and minocycline, indicating that P5 was efficient in the adsorption of tetracycline-type antibiotics. However, the adsorption efficiencies were 2.1% and 1.8% for quinoline and p-nitrophenol, respectively. This behaviour demonstrated that Ps-0.5 has a high selectivity in the adsorption of tetracycline-type antibiotics in comparison with those of quinoline and p-nitrophenol. When P5 was added to the solution, it spontaneously hydrolysed to form the Lewis base of Fe-SH. Thereafter, quinoline and p-nitrophenol were negatively charged in the solution and showed no attachment to the hydrolysed product of  $\text{KFeS}_2$  via electrostatic repulsion, leading to a low removal efficiency. However, tetracycline-type antibiotics were zwitterionic in the solution, and easily cooperated with Lewis base of Fe-SH from  $\text{KFeS}_2$  hydrolysis, resulting in the high level of removal efficiency.

In this study, a strong alkaline solution was employed for  $\text{KFeS}_2$  synthesis, in which the added  $\text{S}^{2-}$  and  $\text{OH}^-$  were consumed in the hydrothermal reaction. However, after the hydrothermal treatment, the used solution comprised portions of  $\text{S}^{2-}$  and  $\text{OH}^-$ , and they can be recycled for the next synthesis

with supplementary KOH and  $\text{K}_2\text{S}$ . Without the supplement-

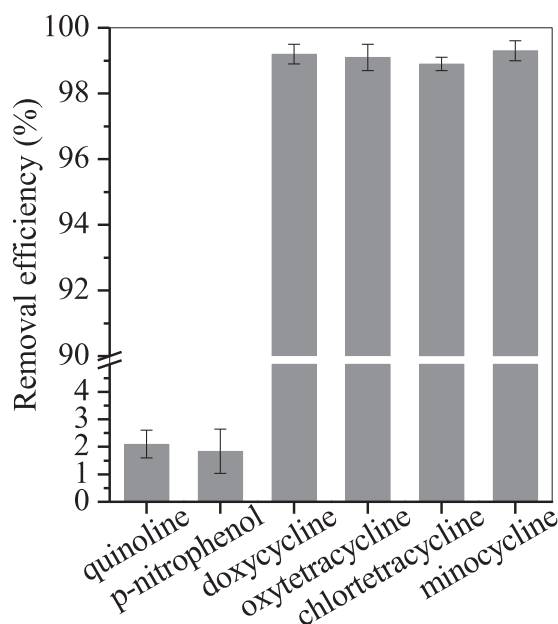


**Fig. 15** Removal efficiencies of quinoline, p-nitrophenol and tetracycline-type antibiotics on P5. For this figure, the experiment was performed with the initial concentration of 20 mg/L at pH 5.5 at room temperature.

tary KOH and  $\text{K}_2\text{S}$ , the rod-shape  $\text{KFeS}_2$  crystal was observed (Fig. 16), but the length was shorted in comparison with that of P5. When KOH and  $\text{K}_2\text{S}$  were added to the residual supernatant, cluster-sharp  $\text{KFeS}_2$  crystals appeared, similar to those of P5. This finding indicates that the residual supernatant can be completely recycled in the subsequent round for  $\text{KFeS}_2$  synthesis.

The synthesis cost of  $\text{KFeS}_2$  is an important parameter for its involvement in wastewater treatment. The synthesis of 1 t  $\text{KFeS}_2$  needs 0.64 t potassium sulphide, 0.12 t potassium hydroxide, 15 h high-temperature steam for heating and 6 kW·h power for drying, with a total cost of US\$890.1 (Table 3). This process comprises the recycling of used alkaline solution and does not generate secondary liquid waste. In addition, ferric trichloride is used as the Fe source in the process, and it can be replaced by waste Fe-rich sludge, which not only reduces the synthesis cost of  $\text{KFeS}_2$  but also eliminates the potential pollution of such Fe-rich sludge. Thus, the synthesis cost of  $\text{KFeS}_2$  was relatively lower than the reported methods with chemical Fe-bearing reagents as raw materials (Boon, 2015; Galembeck and Alves, 1995). By using  $\text{KFeS}_2$ -bearing product (e.g. P5) to treat doxycycline-bearing wastewater, the cost approximates US\$0.37/m<sup>3</sup>, which is lower than that of widely reported adsorbents, e.g. graphene nanosheet

(Rostamian and Behnejad, 2017), metal–organic framework (Xiong et al., 2019), molybdenum disulfide (Chao et al., 2014) and commercial active carbon (Mansour et al., 2018; Xiang et al., 2019), indicating that the application of  $\text{KFeS}_2$  for doxycycline removal is economically acceptable.

With such method, a portion of Fe-rich sludge, e.g. cold-rolling sludge, heavy-metal-bearing electroplating sludge and Al/Si-bearing groundwater sludge, comprised weakly crystallised Fe-bearing compounds. The sludge can be recycled as Fe resource to synthesise  $\text{KFeS}_2$ . This process not only reduces the production of waste Fe-rich sludge but also develops a new product of wastewater treatment. Other sludges include red mud and calcinated mineral slag and contain considerable amounts of crystallised Fe-bearing minerals, e.g. andradite, melanite, pyreneite etc. Such crystallised Fe minerals do not release Fe in strong alkaline solutions and are thereby not involved in the formation of  $\text{KFeS}_2$ . In summary, the abovementioned process can serve as an alternative strategy for the resource utilisation of Fe-rich sludge.

#### 4. Conclusion

The Fe-bearing sludge is commonly generated in the coagulation, Fenton and catalyst process. With the method, such

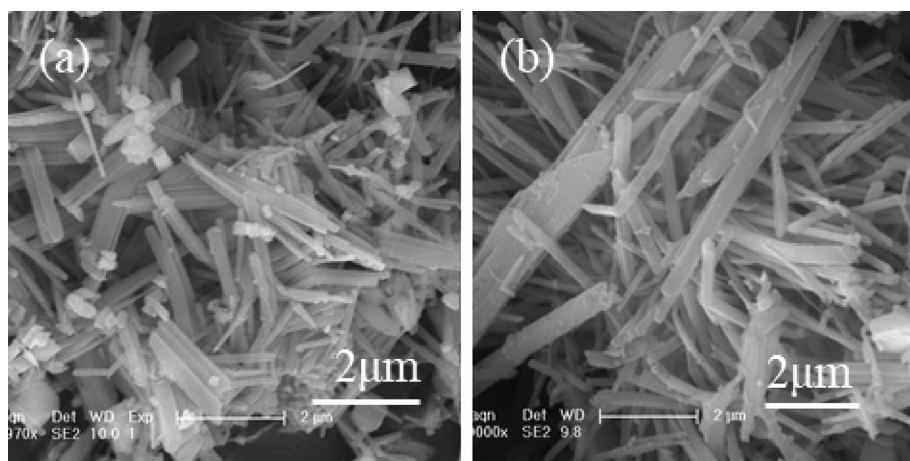


**Fig. 16** SEM images of  $\text{KFeS}_2$ -bearing products synthesised by the recycling of supernatant (a) without and (b) with the addition of 0.5 M KOH and  $\text{K}_2\text{S}$ .

**Table 3** Cost of  $\text{KFeS}_2$  synthesis from groundwater treatment sludge.

	Reagent and processing	Cost	Usage per ton	Subtotal cost (US \$/ton)
Recycling of used alkaline solution for $\text{KFeS}_2$ synthesis	Ferric Trichloride	86.6 US\$/ton	1.02 ton	88.3
	Supplementary Potassium Sulphide	864.2 US\$/ton	0.64 ton	553.1
	Supplementary Potassium Hydroxide	733.3 US\$/ton	0.12 ton	87.9
	Pulping	0.23 US\$/kWsh	0.5 kWsh (total 1 h)	0.1
	Hydrothermal process (Steam Heating)	8.5 US\$/h	15 h	127.5
	Drying	0.23 US\$/kWsh	6 kWsh (total 20 h)	33.1
Total cost				890.1

sludge can be recycled as  $\text{KFeS}_2$ -bearing product via a facile hydrothermal route. During the conversion of sludge to  $\text{KFeS}_2$ , three important reactions occurred. First, the surface Fe of the sludge was dissolved as  $\text{Fe}(\text{OH})_4^-$  in the presence of 2 M KOH. The dissolution intensified with the addition of 5 M KOH. Second, one hydroxyl group of  $\text{Fe}(\text{OH})_4^-$  was replaced by free  $\text{HS}^-$ , and as the replacement reaction continued, a number of intermediate  $\text{Fe}(\text{OH})_3\text{HS}^-$  was produced. Third, the polymerisation reaction of  $\text{Fe}(\text{OH})_3\text{HS}^-$  transpired to release water molecules, and  $(\text{FeS}_2)_n^{n-}$  was the final product. In the hydrothermal system, well-crystallised hematite was also formed from the combination of the adjacent  $\text{FeOOH}$  micro-crystals. Thus, a mixture product of  $\text{KFeS}_2$  and hematite was generated.

The conversion of the sludge to  $\text{KFeS}_2$ -bearing mixture had two remarkable merits, one of which is the reduced cost and space of sludge disposal. In water treatment plant industry, this expenditure was generally considered in the treatment cost of wastewater in the past but can now be regarded as a deduction, effectively saving the operation expense of the water treatment plant. The other merit is the formation of rod-shaped  $\text{KFeS}_2$ -bearing products, which exhibited a desirable hydrolysis performance in the neutral solution and good adsorption capacity for doxycycline. The  $q_m$  of the new adsorbent for doxycycline was 2933.6 mg/g, which is higher than that of raw sludge, pyrite, hematite and PFS. Thus, the new  $\text{KFeS}_2$ -bearing product has a desirable treatment efficiency in doxycycline-bearing wastewater.

#### CRediT authorship contribution statement

**Yu Chen:** Project administration. **Zhihua Wang:** Data curation. **Dongxu Liang:** Validation. **Yanwen Liu:** Validation. **Hongbin Yu:** Supervision. **Suiyi Zhu:** Writing - original draft. **Leilei Zhang:** Software.

#### Declaration of Competing Interest

The authors declare that they have no known competing financial interests or personal relationships that could have appeared to influence the work reported in this paper.

#### Acknowledgments

This work was supported by the National Key Research and Development Program of China (Grant No. 2019YFE0117900), the National Natural Science Foundation of China (Grant Nos. 51878134 and 52070038) and the Science and Technology Program of Jilin Province (Grant No. 20190303001SF).

#### Appendix A. Supplementary material

Supplementary data to this article can be found online at <https://doi.org/10.1016/j.arabjc.2021.103173>.

#### References

- Bousek, J., Schpp, T., Schwaiger, B., Lesueur, C., Fuchs, W., Weissenbacher, N., 2018. Behaviour of doxycycline, oxytetracycline, tetracycline and flumequine during manure up-cycling for fertilizer production. *J. Environ. Manage.* 223, 545–553.
- Ahmad, T., Ahmad, K., Alam, M., 2016. Characterization of water treatment plant's sludge and its safe disposal options. *Procedia Environ. Sci.* 35, 950–955.
- Álvarez-Esmoris, C., Conde-Cid, M., Fernández-Calviño, D., Fernández-Sanjurjo, M.J., Núñez-Delgado, A., Álvarez-Rodríguez, E., Arias-Estévez, M., 2020. Adsorption-desorption of doxycycline in agricultural soils: Batch and stirred-flow-chamber experiments. *Environ. Res.* 186, 109565.
- Boon, J.W., 2015. The crystal structure of chalcopyrite ( $\text{CuFeS}_2$ ) and  $\text{AgFeS}_2$ : The permutoidic reactions  $\text{KFeS}_2 \rightarrow \text{CuFeS}_2$  and  $\text{KFeS}_2 \rightarrow \text{AgFeS}_2$ . *Recl. Trav. Chim. Pays-Bas* 63 (4), 69–80.
- Brigante, M., Avena, M., 2016. Biotemplated synthesis of mesoporous silica for doxycycline removal. Effect of pH, temperature, ionic strength and  $\text{Ca}^{2+}$  concentration on the adsorption behaviour. *Microporous Mesoporous Mater.* 225, 534–542.
- Bronold, M., Pettenkofer, C., Jaegermann, W., 1991. Surface analysis investigations on the reaction of  $\text{FeS}_2$  with alkali metals. *Ber. Bunsenges. Phys. Chem.* 95 (11), 1475–1479.
- Chao, Y., Zhu, W., Wu, X., Hou, F., Xun, S., Wu, P., Ji, H., Xu, H., Li, H., 2014. Application of graphene-like layered molybdenum disulfide and its excellent adsorption behavior for doxycycline antibiotic. *Chem. Eng. J.* 243, 60–67.
- Chen, Y., Li, H., Wang, Z., Tao, T., Hu, C., 2011. Photoproducts of tetracycline and oxytetracycline involving self-sensitized oxidation in aqueous solutions: effects of  $\text{Ca}^{2+}$  and  $\text{Mg}^{2+}$ . *J. Environ. Sci.-China* 23 (10), 1634–1639.
- Chukwudi, C.U., Good, L., 2019. Doxycycline inhibits pre-rRNA processing and mature rRNA formation in *E. coli*. *J. Antibiotics* 72, 225–236.
- Diakonov, I.I., Schott, J., Martin, F., Harrichourry, J.-C., Escalier, J., 1999. Iron(III) solubility and speciation in aqueous solutions. experimental study and modelling: part I. hematite solubility from 60 to 300°C in NaOH–NaCl solutions and thermodynamic properties of  $\text{Fe}(\text{OH})_4^-(\text{aq})$ . *Geochim. Cosmochim. Acta* 63 (15), 2247–2261.
- Dunnwald, J., Otto, A., 1989. An investigation of phase transitions in rust layers using raman spectroscopy. *Cheminform.* 29 (9), 1167–1176.
- EPA, 2011. Drinking Water Treatment Plant Residuals Management Technical Report, EPA Washington, DC, USA.
- Galembeck, A., Alves, O.L., 1995. Morphological investigations on iron potassium sulfide  $\text{KFeS}_2$ : grinding effect on thermal behavior. *Mater. Lett.* 23 (1), 133–138.
- Gao, Y., Li, Y., Zhang, L., Huang, H., Hu, J., Shah, S.M., Su, X., 2012. Adsorption and removal of tetracycline antibiotics from aqueous solution by graphene oxide. *J. Colloid Interface Sci.* 368 (1), 540–546.
- Gui, J., Devine, T.M., 1993. The influence of sulfate ions on the surface enhanced raman spectra of passive films formed on iron. *Corros. Sci.* 36 (3), 441–462.
- Guy, J.K., Spann, R.E., Martin, B.R., 2008. Solid state ion exchange chemistry of the solid solution  $\text{K}_x\text{Rb}_{1-x}\text{FeS}_2$ . *Solid State Ionics* 179 (11–12), 409–414.
- Han, S.C., Park, W.B., Sohn, K.-S., Pyo, M., 2020. Mixed anion/cation redox in  $\text{K}_{0.78}\text{Fe}_{1.60}\text{S}_2$  for a high-performance cathode in potassium ion batteries. *Inorg. Chem. Front.* 7 (10), 2023–2030.
- Honma, H., Nakata, M., Kobayashi, K., 2003. Formation Condition of Erdite in System  $\text{FeCO}_3$ -NaHS Solution at 150°C. *Bulletin of Tokyo Gakugei Univ.* 55, 39–44.
- Hu, T., Wang, H., Ning, R., Qiao, X., Liu, Y., Dong, W., Zhu, S., 2020. Upcycling of Fe-bearing sludge: preparation of erdite-bearing particles for treating pharmaceutical manufacture wastewater. *Sci. Rep.* 10 (1), 1–10.
- Jianmin, Z., 1994. Ferrihydrite: surface structure and its effects on phase transformation. *Clays Clay Miner.* 42 (6), 737–746.

- Lassin, A., Piantone, P., Crouzet, C., Bodéan, F., Blanc, P., 2014. Estimated thermodynamic properties of NaFeS<sub>2</sub> and erdite (NaFeS<sub>2</sub>·2H<sub>2</sub>O). *Appl. Geochem.* 45 (4), 14–24.
- Li, S., Wang, W., Liu, Y., Zhang, W.-X., 2014. Zero-valent iron nanoparticles (nZVI) for the treatment of smelting wastewater: a pilot-scale demonstration. *Chem. Eng. J.* 254, 115–123.
- Li, X., Graham, N.J.D., Deng, W., Liu, M., Liu, T., Yu, W., 2020a. The formation of planar crystalline flocs of  $\gamma$ -FeOOH in Fe(II) coagulation and the influence of humic acid. *Water Res.* 185, 116250.
- Li, Y., Tian, X., He, X., Liu, Y., Ye, J., Wei, Y., 2020b. Comprehensive reutilization of iron in iron ore tailings: preparation and characterization of magnetic flocculants. *Environ. Sci. Pollut. Res.* 27 (29), 37011–37021.
- Li, Y., van Santen, R.A., Weber, T., 2008. High-temperature FeS–FeS<sub>2</sub> solid-state transitions: Reactions of solid mackinawite with gaseous H<sub>2</sub>S. *J. Solid State Chem.* 181 (11), 3151–3162.
- Liu, J., Yu, Y., Zhu, S., Yang, J., Song, J., Fan, W., Yu, H., Bian, D., Huo, M., 2018. Synthesis and characterization of a magnetic adsorbent from negatively-valued iron mud for methylene blue adsorption. *PLoS ONE* 13 (2), e0191229.
- Liu, Y., Khan, A., Wang, Z., Chen, Y., Zhu, S., Sun, T., Liang, D., Yu, H., 2020. Upcycling of Electroplating Sludge to Prepare Erdite-Bearing Nanorods for the Adsorption of Heavy Metals from Electroplating Wastewater Effluent. *Water* 12 (4), 1027.
- Mansour, F., Al-Hindi, M., Yahfoufi, R., Ayoub, G.M., Ahmad, M. N., 2018. The use of activated carbon for the removal of pharmaceuticals from aqueous solutions: a review. *Rev. Environ. Sci. Bio/Technol.* 17 (1), 109–145.
- Mazzetti, L., Thistlethwaite, P.J., 2002. Raman spectra and thermal transformations of ferrihydrite and schwertmannite. *J. Raman Spectrosc.* 33 (2), 104–111.
- Mooheng, P., Phenrat, T., 2019. Acid-Assisted Recycling of Iron Hydroxide Sludge as a Coagulant for Metalworking Fluid Wastewater Treatment. *Waste Biomass Valorizat.* 10, 3635–3645.
- Neth, N., Carlin, C.M., Keen, O.S., 2017. Doxycycline transformation and emergence of antibacterially active products during water disinfection with chlorine. *Environ. Sci. Water Res. Technol.* 3 (6), 1086–1094.
- Ngatenah, S.N.I., Kutty, S.R.M., Isa, M.H., 2010. Optimization of heavy metal removal from aqueous solution using groundwater treatment plant sludge (GWTPS). In: *International Conference on Environment Penang, Malaysia*, pp. 1–9.
- Osman, S.B.S., Iqbal, F., 2014. Possible stabilization of sludge from groundwater treatment plant using electrokinetic method. *Appl. Mech. Mater.* 567 (419), 110–115.
- Prashanth, V., Jayasree, P., Rajput, P. and Remya, N.r., 2021. Solar photocatalysis and its application for emerging contaminant removal from wastewater. *Advanced Oxidation Processes for Effluent Treatment Plants*. Shah, M. P., Elsevier, pp. 69–85.
- Qiang, Z., Chang, J.-H., Huang, C.-P., 2003. Electrochemical regeneration of Fe<sup>2+</sup> in Fenton oxidation processes. *Water Res.* 37 (6), 1308–1319.
- Qu, Z., Dong, G., Zhu, S., Yu, Y., Huo, M., Xu, K., Liu, M., 2020. Recycling of groundwater treatment sludge to prepare nano-rod erdite particles for tetracycline adsorption. *J. Cleaner Prod.* 257, 120462.
- Qu, Z., Wu, Y., Zhu, S., Yu, Y., Huo, M., Zhang, L., Yang, J., Bian, D., Wang, Y., 2019. Green synthesis of magnetic adsorbent using groundwater treatment sludge for tetracycline adsorption. *Engineering* 5 (5), 880–887.
- Rostamian, R., Behnejad, H., 2017. Insights into doxycycline adsorption onto graphene nanosheet: a combined quantum mechanics, thermodynamics, and kinetic study. *Environ. Sci. Pollut. Res. Int.* 25 (4), 1–10.
- Rupa Ranjani, P., Anjana, P.M., Rakhi, R.B., 2021. Solvothermal synthesis of CuFeS<sub>2</sub> nanoflakes as a promising electrode material for supercapacitors. *J. Storage Mater.* 33, 102063.
- Simonetti, S., Damiani, D., Brizuela, G., Juan, A., 2006. Sulfur adsorption on the goethite (110) surface. *Surf. Rev. Lett.* 13 (4), 387–395.
- Sun, M., Yan, L., Zhang, L., Song, L., Guo, J., Zhang, H., 2019. New insights into the rapid formation of initial membrane fouling after in-situ cleaning in a membrane bioreactor. *Process Biochem.* 78, 108–113.
- Tang, R., Wang, Z., Muhammad, Y., Shi, H., Liu, K., Ji, J., Zhu, Y., Tong, Z., Zhang, H., 2021. Fabrication of carboxymethyl cellulose and chitosan modified Magnetic alkaline Ca-bentonite for the adsorption of hazardous doxycycline. *Colloids Surf., A* 610, 125730.
- Thomas, V., Long, I.I., Thomas, M., Loehr, 1970. Possible determination of iron coordination in nonheme iron proteins using laser-Raman spectroscopy. Rubredoxin. *J. Am. Chem. Soc.* 92 (21), 6384–6386.
- Wang, Z., Liu, Y., Qu, Z., Su, T., Khan, A., 2021. In situ conversion of goethite to erdite nanorods to improve the performance of doxycycline hydrochloride adsorption. *Colloids Surf., A* 614, 126132.
- Xiang, Y., Xu, Z., Wei, Y., Zhou, Y., Yang, X., Yang, Y., Yang, J., Zhang, J., Luo, L., Zhou, Z., 2019. Carbon-based materials as adsorbent for antibiotics removal: Mechanisms and influencing factors. *J. Environ. Manage.* 237, 128–138.
- Xiong, W., Zeng, Z., Li, X., Zeng, G., Xiao, R., Yang, Z., Xu, H., Chen, H., Cao, J., Zhou, C., Qin, L., 2019. Ni-doped MIL-53(Fe) nanoparticles for optimized doxycycline removal by using response surface methodology from aqueous solution. *Chemosphere* 232, 186–194.
- Yang, K., Wang, Y., Lu, C., Yang, X., 2018. Ovalbumin-directed synthesis of fluorescent copper nanoclusters for sensing both vitamin B1 and doxycycline. *J. Lumin.* 196, 181–186.
- Zaidi, S., Chaabane, T., Sivasankar, V., Darchen, A., Maachi, R., Msagati, T., 2019. Electro-coagulation coupled electro-flotation process: Feasible choice in doxycycline removal from pharmaceutical effluents. *Arab. J. Chem.* 12 (8), 2798–2809.
- Zhang, H., Sun, M., Song, L., Guo, J., Zhang, L., 2019a. Fate of NaClO and membrane foulants during in-situ cleaning of membrane bioreactors: Combined effect on thermodynamic properties of sludge. *Biochem. Eng. J.* 147, 146–152.
- Zhang, L., Zhang, M., Guo, J., Zheng, J., Chen, Z., Zhang, H., 2019b. Effects of K<sup>+</sup> salinity on the sludge activity and the microbial community structure of an A<sub>2</sub>O process. *Chemosphere* 235, 805–813.
- Zhu, S., Fang, S., Huo, M., Yu, Y., Chen, Y., Yang, X., Geng, Z., Wang, Y., Bian, D., Huo, H., 2015. A novel conversion of the groundwater treatment sludge to magnetic particles for the adsorption of methylene blue. *J. Hazard. Mater.* 292, 173–179.
- Zhu, S., Li, T., Wu, Y., Chen, Y., Su, T., Ri, K., Huo, Y., 2020a. Effective purification of cold-rolling sludge as iron concentrate powder via a coupled hydrothermal and calcination route: From laboratory-scale to pilot-scale. *J. Cleaner Prod.* 276, 124274.
- Zhu, S., Lin, X., Dong, G., Yu, Y., Yu, H., Bian, D., Zhang, L., Yang, J., Wang, X., Huo, M., 2019a. Valorization of manganese-containing groundwater treatment sludge by preparing magnetic adsorbent for Cu(II) adsorption. *J. Environ. Manage.* 236, 446–454.
- Zhu, S., Liu, Y., Huo, Y., Chen, Y., Qu, Z., Yu, Y., Wang, Z., Fan, W., Peng, J., Wang, Z., 2019b. Addition of MnO<sub>2</sub> in synthesis of nano-rod erdite promoted tetracycline adsorption. *Sci. Rep.* 9 (1), 1–12.
- Zhu, S., Wu, Y., Qu, Z., Zhang, L., Yu, Y., Xie, X., Huo, M., Yang, J., Bian, D., Zhang, H., 2020b. Green synthesis of magnetic sodalite sphere by using groundwater treatment sludge for tetracycline adsorption. *J. Cleaner Prod.* 247, 119140.